APR1400 MFLB Safety Analysis using MARS-KS CTF Sub-channel Analysis Module and Parallelization Challenges

N.H. Hoang*, Y.S. Kim, Y.K. Kwack, S.H. Bae, S.K. Sim
Environment and Energy Technology Inc., R&D Building 2, 99 Gajeong-ro, Yuseong-gu, Daejeon, 34115, Korea
* Corresponding author: *hien@en2t.com*

1. Introduction

Toward the full-core thermal-hydraulic and safety analysis of nuclear power plants, CTF sub-channel analysis code, an improved version of COBRA-TF code, has been recently coupled with MARS-KS code by implicit coupling of pressure matrices [1]. One of the great features of the improved CTF code is a capability of parallel processing that allows full-core analysis to have more realistic evaluation of thermal-hydraulic behaviors of the core, especially the fuel region [2]. The coupled MARS-KS code is now parallelized after its serial processing is improved.

In this paper, the applicability and performance of the serially coupled MARS-KS code is evaluated. The main feedwater line break (MFLB) accident of the reference plant, APR1400, is specifically analyzed with the coupled MARS-KS code for the evaluation. Besides the code capability, the transient behavior of the DNBR, an important thermal limit of nuclear fuel, was addressed to highlight the DNBR predictability of the improved MARS-KS code. Finally, challenges of the parallelization of the coupled MARS-KS code with CTF full-core sub-channel module for the full-core analysis are also discussed in this paper.

2. APR1400 Main Feedwater Line Break

In this study, the limiting MFLB with the break size of 0.0372 m^2 downstream of the check valves with assumed Loss-Of-Offside-Power (LOOP) was analyzed. The downstream break has potential to establish reverse flow from the nearest steam generator (so-called affected SG), and thus resulting in a rapid RCS heat-up and pressurization due to rapid depletion of the affected SG liquid inventory.

The MARS-KS nodalization used for the APR1400 MFLB is shown in Figure 1. This nodalization includes a 3D vessel component that is modeled by the CTF module. The reactor core is divided into six sections and a total of 32 sub-channels. Crossflow across the sub-channels is simulated by a total of 28 gaps. Seven lumped heaters and six lumped conductors of the CTF module are used to simulate a total of 241 fuel assemblies. The power supplying heat to all the heaters is assumed to have a bottom cosine-shape axial

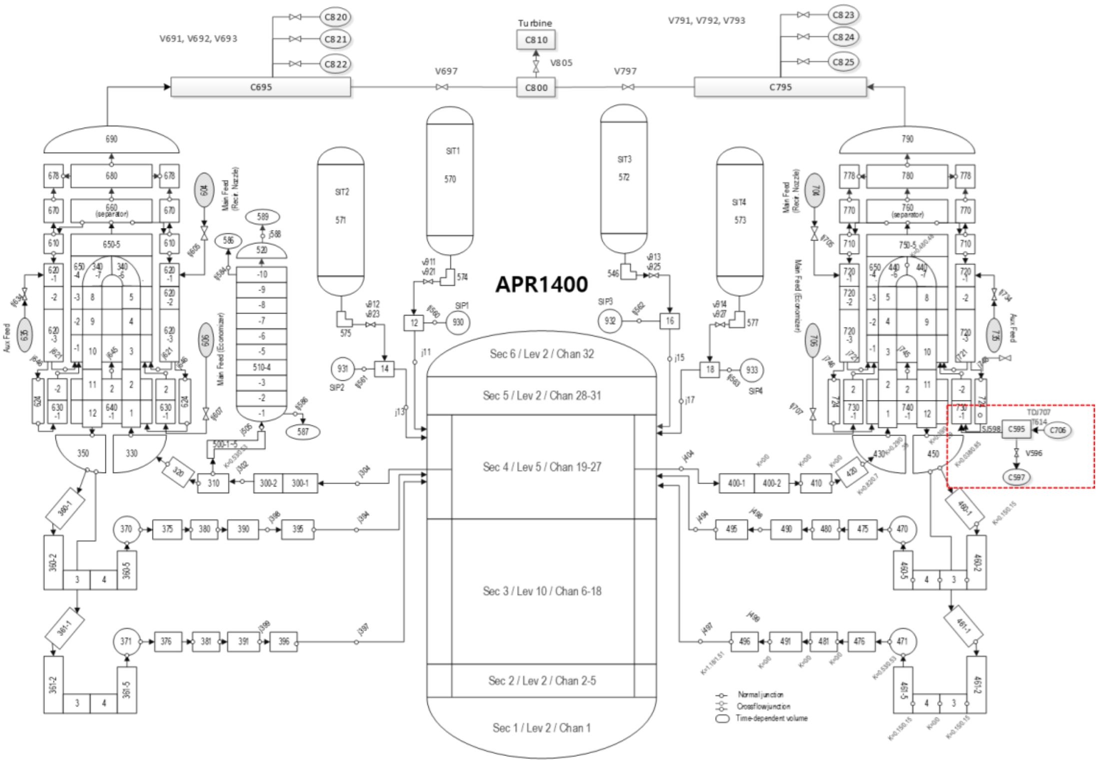

Figure 1. APR1400 MFLB nodalization

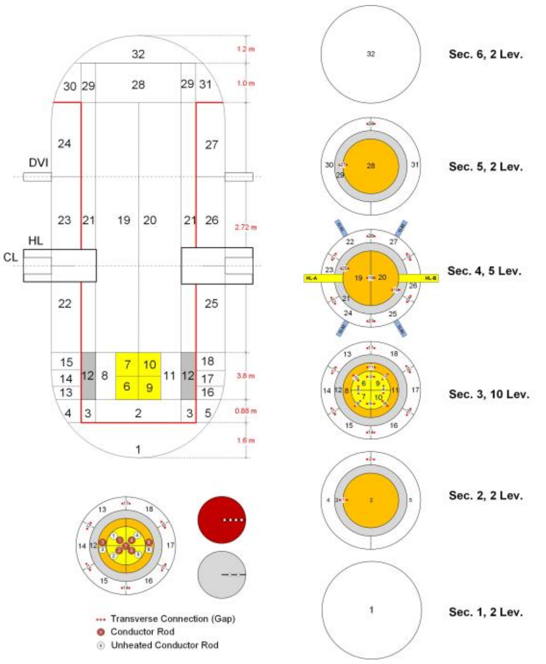

Figure 2. Vessel component

distribution. And a radial peaking factor of 1.33 was assumed to heater 7 which simulates the hot pin. Details of the 3D vessel component is shown in Figure 2. The RCS loops and secondary systems of the plant are modeled by MARS-KS 1D components.

The initial and boundary conditions of the APR1400 MFLB accident analysis were conservatively set based on the limiting conditions for operation (LCOs) of the APR1400 Final Safety Analysis Report (FSAR) [3] as shown in Table 1. The auxiliary feedwater supply system (AFWS) was not available for the affected SG side. The Henry-Fauske critical flow model and ANS-73 decay heat curve with 20% conservative uncertainty were applied. The sequence of events of the transient is listed in Table 2.

Table 1. APR1400 MFLB Initial & boundary conditions

Parameter	FSAR [3]	MARS/CTF
Thermal power, MWt	4062.66	4062.66
Core inlet temp. (K)	569.25	569.11
Core outlet temp. (K)	-	604.18
Core inlet flow (kg/s)	19,344	19,344
PRZ pressure (MPa)	15.65	15.65
PRZ volume (m^3)	39.91	39.91
Main steam flow (kg/s)	-	1143
SG pressure (MPa)	-	7.7
SG water level (m)	-	12.53
SG water inventory (kg)	97,046	97,046
CEA worth at trip (%Δρ)	-8.0	-8.0
MTC (10^{-4} %Δρ/°C)	0	0
Doppler reactivity	Least negative	Least negative

Table 2. APR1400 MFLB sequence of events

MARS/ CTF	FSAR	Events	Setpoints
0.0	0.0	Break initiates Loss of feedwater to SGs	0.0372 m^2
33.62	26.38	High PRZ press. signal	16.98 MPa
34.37	27.13	Reactor trip breakers open LOOP Turbine valve closes	0.75s delay
35.8	27.37	POSRV opens	17.37 MPa
37.0	24.43	Maximum RCS pressure	18.54 MPa
38.0	33.25	POSRV closes	15.62 MPa
42.2	54.64	AFWS actuation signal	5% SG lev.
43.2	29.95	MSSVs open (unaff. SG)	8.59 MPa
49.0	35.63	Maximum SG pressure	8.8 MPa
67.0	57.04	MSSVs close	7.73 MPa
103.7	116.1	AFW inject. (unaff. SG)	41.01 kg/s
169.9	159.1	MSIVs closing sig. (P_{SG})	5.17 MPa
176.4	165.6	MSIVs close	
452.0	401.4	MSSVs re-open	5.89 MPa
479.0	457.3	POSRV opens	17.37 MPa
481.4	459.7	POSRV closes	15.62 MPa
1800	1800	End of simulation	

At the break, the subcooled feedwater (FW) to the affected SG was lost through the break (see Fig 3), causing an increase of SG temperature and a rapid decrease of SG water level as shown in Figure 4. This resulted in a rapid RCS heat-up and pressurization as shown in Figures 5-6, followed by a reactor trip due to the high pressurize (PRZ) pressure signal. As shown in Figure 7, the transient power was decreased at the beginning due to the increasing fuel and moderator temperatures and least negative fuel and moderator temperature coefficients assumed, and then sharply dropped after the reactor trip. Following that moment, the behaviors of POSRVs, MSSVs, and MSIVs were controlled by the transient PRZ and SG pressures (see Table 2). When the SG level reduces below 5%, the AFWS started to inject FW to the unaffected SG.

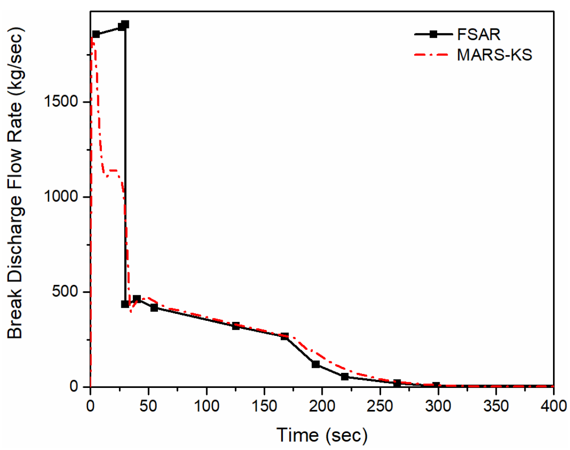

Figure 3. Break flow

In comparison with the FSAR results, the break flow is lower at the beginning. It therefore took little more time, about 7 seconds, to reach the high PRZ pressure setpoint of 16.98 MPa which caused the reactor trip. And the opening and closing of the POSRV were delayed. After the break initiation, the water level of the affected SG rapidly reduced, and hence more heat seemed to be delivered to the unaffected SG compared to the FSAR results. This caused the water level of this unaffected SG lower than the FSAR result as well as the early operation of the AFWS. The faster reduction of the unaffected SG level is the reason for the higher RCS temperature and pressure that were established by the unbalance of heat generation by the fuel and heat removal by the SGs after about 350 seconds as shown in Figures 4–6.

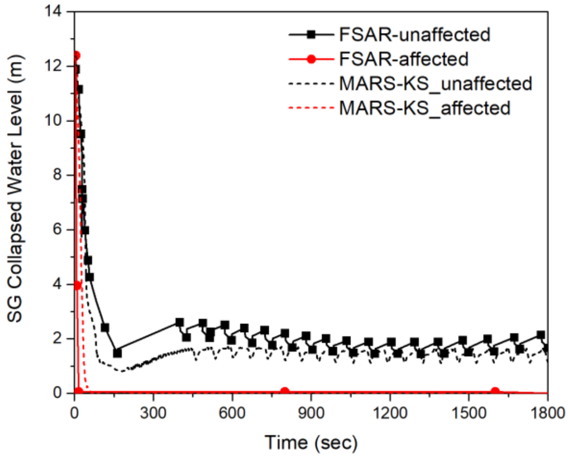

Figure 4. SG collapsed water level

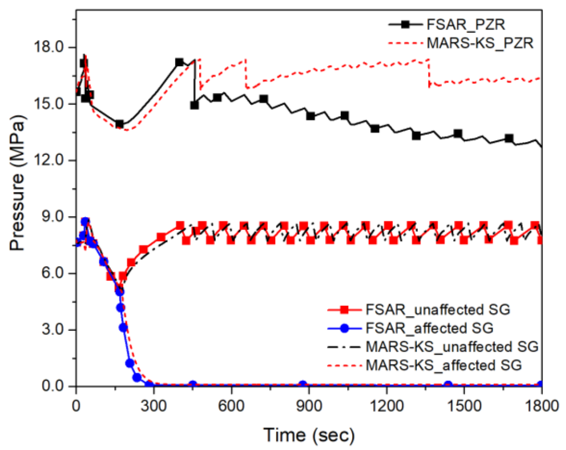

Figure 5. System pressure

The transient DNBR of the hot pin, in connection to the RCS heat-up, also showed a delay compared with the FSAR result, as shown in Figure 8. The lower break flow at the beginning led to a slower rate of core heat-up. The local heat flux of the hot pin therefore increased slowly resulting in the delay of the transient DNBR. In addition, the minimum DNBR value predicted by the MARS-KS CTF sub-channel module is slightly lower than FSAR but still higher than the APR1400 DNBR limit of 1.29. It is reminded that the minimum DNBR depends on the CHF correlation used. In this study, the Groeneveld look-up table was used whereas it was KCE-1 CHF correlation for the APR1400 FSAR. It should be noted that the FSAR evaluated DNBR separately by the design sub-channel thermal-hydraulics code, CETOP, using conservative CESEC-III safety analysis transient outputs to evaluate thermal margins, including DNBR. Thus, differences in the safety analysis methodology between the APR1400 FSAR and MARS-KS should be further identified.

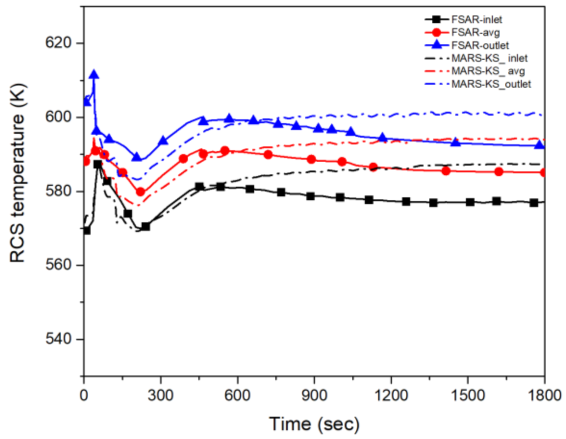

Figure 6. RCS temperature

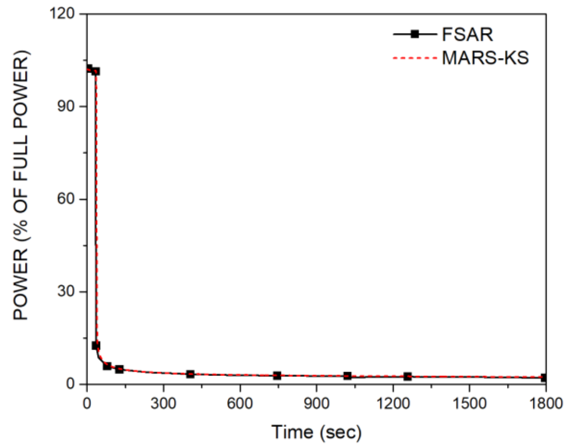

Figure 7. Reactor power

It can be highlighted, through the analytical results presented above, that the MARS-KS code with CTF sub-channel analysis module has adequate capability to predict the MFLB transient of the APR1400 plant, especially for the transient DNBR. The transient predictions of the MARS-KS can be improved by considering different 3D vessel nodalizations. The current vessel nodalization with a limited number of sub-channels and lumped heaters/conductors seems insufficient in simulating flow mixing at the lower plenum and power distributions of the fuel. The flow mixing would affect the flow and temperature at the core and hot legs, resulting in different heat removal by the SGs. And the power distributions would strongly affect the DNBR.

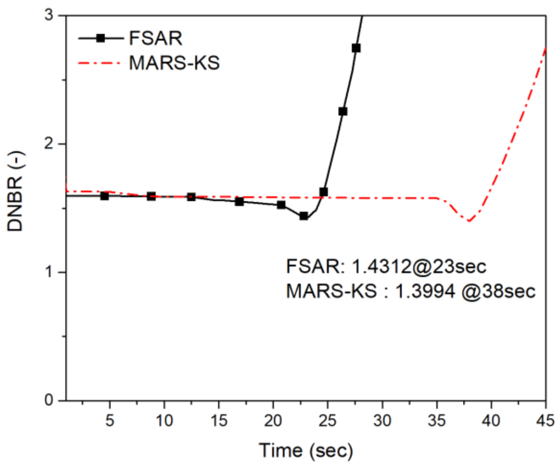

Figure 8. Transient DNBR at the hot pin

3. Challenges for Parallelization of the MARS-KS

It is clear that to improve the prediction of the coupled MARS-KS code we need more detailed vessel nodalization with a large number of sub-channels, gaps, heaters, and conductors. However, computation with such a nodalization consumes extensive computer resources and time. To overcome this difficulty, parallelization of the MARS-KS code is required. This could pave a promising way of full-core thermal-hydraulic simulations, especially for the innovative small and modular reactor (SMRs) and micro reactors (MRs). However, it would be also very challenging for the parallelization of the MARS-KS code especially on the Windows system.

The CTF code currently uses a relatively standard Single Program Multiple Data (SPMD) strategy targeting distributed memory "multiple instruction multiple data" (MIMD) platform and domain decomposition for parallel processing [2]. During the parallelization of the coupled MARS-KS code, CTF Windows version with parallel processing has been successfully tested against the test of 2x2 BWR fuel assemblies (FAs), which were divided into 4 domains with a total of 1764 cells as shown in Figure 9.

In the coupled MARS-KS code, the same method of parallel processing has been applied to utilize the advantage of the CTF code. The MARS-KS 1D system module works as the master process, running in serial processing mode and giving instructions to the CTF module that is in parallel processing mode. In this way, it minimized the code modification for the parallelization. What we mostly have to focus is the MARS-KS 1D system module and its interfaces with the 3D CTF module. Due to the coupling of MARS-KS and CTF 1D/3D modules, the calculations performed by two modules are interchanged in the MARS-KS code. It is therefore necessary to optimize the MARS-KS structure first to separate the calculations of two modules as much as possible.

There are some challenges in parallelization of the 1D/3D interface couplings between the MARS-KS 1D system and CTF 3D modules. However, this will be a start of developing virtual technology for the future self-controlling and self-driving SMRs and MRs.

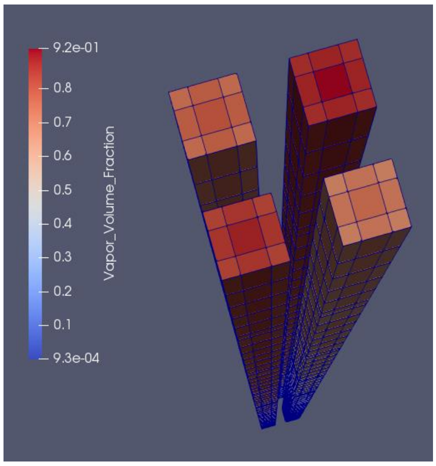

Figure 9. CTF parallel calculation for 2x2 BWR FAs

4. Conclusions

The coupled MARS-KS code with CTF sub-channel analysis module showed realistic capability of predicting the postulated MFLB accident for the APR1400 plant. Thus, MARS-KS can be directly used to independently review the transient and accident analyses of the FSAR and transient DNBR during non-LOCA design basis accidents. The coupled MARS-KS code with CTF sub-channel analysis module is an example of the multi-physics and multi-scaled code integration. Currently, MARS-KS is upgrading the parallel processing capability for the full core analysis. There is a challenge for the realistic system safety analysis code to expand its capability for full core modeling, especially for the SMRs and MRs, using parallel processing technology as a part of the integrated multi-physics and multi-scaled computational methods.

REFERENCES

[1] N.H. Hoang, Y.K. Kwack, S.H. Bae, Y.S. Kim, S.K. Sim, Improvement of MARS-KS sub-channel module using CTF code, Nucl. Eng. Design, Vol. 358, 119431, 2020.
[2] R.K. Salko, R.C. Schmidt, M.N. Avramova, Optimization and parallelization of the thermal-hydraulic subchannel code CTF for high-fidelity multi-physics applications, Annu. Nucl. Energy, Vol. 84, pp. 329-344, 2015.
[3] Korea Hydro & Nuclear Power Company, "Final Safety Analysis Report, Shin-Kori Units 3&4", 2015.